Acene-Containing Donor–Acceptor Conjugated Polymers: Correlation between the Structure of Donor Moiety, Charge Carrier Mobility, and Charge Transport Dynamics in Electronic Devices

ARTICLE *in* MACROMOLECULES · MAY 2014

Impact Factor: 5.8 · DOI: 10.1021/ma500733y

8 AUTHORS, INCLUDING:

Tae Wan Lee
Korea University
49 PUBLICATIONS **411** CITATIONS
SEE PROFILE

Min Ju Cho
Korea University
140 PUBLICATIONS **1,278** CITATIONS
SEE PROFILE

Dong Hoon Choi
Korea University
283 PUBLICATIONS **2,514** CITATIONS
SEE PROFILE

Macromolecules

Article

pubs.acs.org/Macromolecules

Acene-Containing Donor–Acceptor Conjugated Polymers: Correlation between the Structure of Donor Moiety, Charge Carrier Mobility, and Charge Transport Dynamics in Electronic Devices

Gi Eun Park,[†] Jicheol Shin,[†] Dae Hee Lee,[†] Tae Wan Lee,[†] Hyunseok Shim,[‡] Min Ju Cho,[†] Seungmoon Pyo,*[,‡] and Dong Hoon Choi*[,†]

[†]Department of Chemistry, Research Institute for Natural Sciences, Korea University, 5 Anam-dong, Sungbuk-gu, Seoul 136-701, South Korea

[‡]Department of Chemistry, Konkuk University, 1 Hwayang-dong, Kwangjin-gu, Seoul 143-701, South Korea

Supporting Information

ABSTRACT: We synthesized five different donor–acceptor (D–A) conjugated polymers bearing diketopyrrolopyrrole (DPP) acceptors and acene donors in the repeating groups via the Suzuki and Stille coupling methods. To investigate the effect of acene donor moieties on static and dynamic charge transport properties, pyrene, naphthodithiophene, benzodithiophene, dithieno[3,2-*b*:2′,3′-*d*]thiophene (DTT), and thieno[3,2-*b*]thieno[2′,3′:4,5]thieno[2,3-*d*]thiophene (TTTT) were selected and introduced into the structure of the polymer repeating group. Among the five polymers, the polymer PDPPTTTT bearing TTTT donor units exhibited the highest hole mobility, ~3.2 $cm^2\ V^{-1}\ s^{-1}$ ($I_{on}/I_{off} > 10^6$) in the thin film transistors. The five polymers had different mobilities and exhibited different charge transport dynamic responses. The response was investigated by applying a pulsed bias to thin film transistors loaded with a resistor. The resistor loaded (RL) inverter made of PDPPTTTT operates well, maintaining a fairly high switching voltage ratio at a relatively high frequency. The PDPPTTTT-based RL inverter also had the fastest switching behavior with a relatively small decay time of 1.86 ms. From this study, the structure of the donor moiety in the D–A conjugated polymer was found to strongly affect the optical property, internal morphology of the polymer film, charge carrier mobility, and charge transport dynamics in electronic devices.

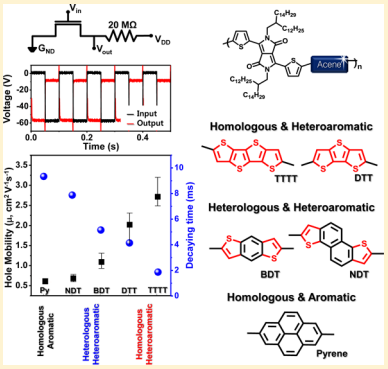

INTRODUCTION

Conjugated polymers for thin-film transistors (TFTs) have attracted significant attention because of their easy structure modification, solution processability, and cheap device solution fabrication such as spin-coating, dip-coating, and drop-casting.[1] Among the numerous semiconducting materials of TFTs reported in the literature, donor–acceptor (D–A) alternating copolymers are the most promising and attractive materials for electronic and optoelectronic applications in recent years.[2−5]

D–A conjugated polymers show highly effective electron delocalization along the polymer chains owing to their push–pull structures. In addition, these copolymers show strong intra- and intermolecular interactions, which facilitate $\pi-\pi$ stacking, thereby improving polymer chain ordering and making the charge hopping behavior more facile in the solid matrix.[2] Because of these advantages, designing specific conjugated polymers by selecting donor and acceptor moieties requires special attention to certain properties such as electron-donating or -accepting capability, planarity, stability, and efficient tailoring of electronic properties through chemical structure modification.[3] Recently, many studies have proven that donor units in the repeating groups of conjugated polymers can affect the effective conjugation, polymer chain geometry, and solid state morphology to modulate charge carrier mobility.[4,5]

Acene molecules are rigid and perfectly planar, which is highly effective for inducing strong $\pi-\pi$ interactions between the polymer chains. Moreover, the interchain interaction in the film is highly promoted to reduce the $\pi-\pi$ stacking distance between the polymer chains, and this is beneficial for charge transport in films.[6−13]

Acene derivatives can be classified into three categories depending on the type of component: homologous aromatic, homologous heteroaromatic, and heterologous heteroaromatic. Naphthalene, pyrene (Py), and anthracene are included in the homologous aromatic fused acenes.[6] Heterologous heteroaromatic fused acenes such as naphthodithiophene (NDT)[7−9] and benzodithiophene (BDT)[10,11] are composed of benzene and thiophene rings. On the other hand, dithieno[3,2-*b*:2′,3′-*d*]thiophene (DTT)[12,13] and thieno[3,2-*b*]thieno[2′,3′:4,5]-thieno[2,3-*d*]thiophene (TTTT)[14,15] are homologous heteroaromatic fused acenes. The rigid and planar fused thiophenes

Received: April 8, 2014
Revised: May 15, 2014
Published: May 30, 2014

   dx.doi.org/10.1021/ma500733y | *Macromolecules* 2014, 47, 3747–3754

exhibits relatively stronger electron donability and their characteristics can induce highly promoted charge transport properties in conjugated polymers.[16,17]

However, regardless of these advantages, a big obstacle for solution processing is often encountered, i.e., poor solubility of the polymer even at a low molecular weight. When the plain acene donor moiety is introduced into the repeating unit of D−A conjugated polymer, the poor solubility is often observed. Even during polymerization, some of the polymer can be precipitated out of the reaction mixture. This undesired shortcoming can be overcome by controlling the length of the side chain tethered to the acceptor monomer. Therefore, to use acene monomers in D−A conjugated polymers, side chain engineering is required as it helps the feasibility of solution processing and promotes crystallinity of the polymers.[18] In this sense, a diketopyrrolopyrrole (DPP) moiety is advantageous to have two long and bulky side chains in two lactam rings. Thus, without attaching side chain molecules to the acene donor moiety, good solubility of the polymer could be achieved in organic solvents.

In this study, we designed and synthesized five different D−A conjugated polymers. As an acceptor, we selected DPP unit with a long and bulky dodecylhexadecyl side chain to form the D−A repeating group. To investigate the effect of acene donor moieties on static and dynamic charge transport properties, Py, NDT, BDT, DTT, and TTTT were introduced into the structure of the polymer repeating group.

Optical, thermal, and electrochemical properties of the polymers were investigated in detail. The morphologies of the thin films were characterized by atomic force microscopy (AFM) and grazing incidence X-ray diffraction (GI-XRD). Among the TFTs made of five acene-containing polymers, the TFT composed of thermally annealed PDPPTTTT film exhibited the highest hole mobility of ∼3.2 $cm^2\ V^{-1}\ s^{-1}$ ($I_{on}/I_{off} > 10^6$), which can be supported by GI-XRD measurement.

Eventually, we fabricated a simple resistor-loaded (RL) inverter and performed experiments for monitoring charge transport dynamics, which is of crucial importance in practical transistor devices.[19] It was found that a higher mobility polymer could exhibit better ON/OFF switching behavior at a high frequency bias voltage. The PDPPTTTT-based RL-inverter device displayed a short rising time (<1 ms) and a decay time of 1.86 ms, which is much smaller than the times observed in RL inverters made from the other four acene-containing polymers.

EXPERIMENTAL SECTION

Materials and Synthesis. All reagents were purchased from Sigma-Aldrich, TCI, and Acros Co. and used without further purification, unless otherwise stated. Reagent grade solvents used in this study were freshly dried under standard distillation methods. Bis(trimethylstannyl)TTTT, bis(trimethylstannyl)DTT, bis-(trimethylstannyl)BDT, and 2,7-bis[4,4,5,5-tetramethyl-1,3,2-dioxaborolan-2-yl]pyrene were synthesized by the literature methods.[6,9−11] PDPPNDT was also synthesized according to previous literature.[7] The detailed synthetic procedures and characterization data for five conjugated polymers are described in the Supporting Information.

Instruments. Elemental analyses were performed on an EA1112 (Thermo Electron Corp., West Chester, PA) elemental analyzer. The molecular weights of the polymers were determined by gel permeation chromatography (GPC) (Waters GPC, Waters 515 pump, Waters 410 RI, 2× PLgel Mixed-B) using a polystyrene standard and $CHCl_3$ as the eluent (T = 35 °C) at the Korean Polymer Testing and Research Institute, Seoul, Korea.

The thermal properties of the five polymers were studied under a nitrogen atmosphere on a Mettler 821e differential scanning calorimeter (DSC) (Mettler, Greifensee, Switzerland). Thermal gravimetric analysis (TGA) was performed on a Mettler TGA50 instrument (temperature rate: 10 °C min^{-1} under nitrogen).

The redox properties of the five polymers were examined by cyclic voltammetry (CV) (EA161 eDAQ). The polymer thin films were coated on a Pt wire using chloroform. The electrolyte solution was 0.10 M tetrabutylammonium hexafluorophosphate (Bu_4NPF_6) in freshly dried acetonitrile. Ag/AgCl and Pt wire (0.5 mm in diameter) electrodes were used as the reference electrode and counter electrode, respectively. The scan rate was 20 mV s^{-1}.

GI-XRD measurements were performed at the 9A (U-SAXS) beamline (energy = 11.26 keV, pixel size = 79.6 μm, wavelength = 1.101 Å, at the Pohang Accelerator Laboratory (PAL)). The measurements were obtained over a scanning interval of 2θ between 0° and 20°. The variable q_{xy} and q_z are the components of the scattering vector parallel and perpendicular to the substrate, respectively, where $q = (4\pi/\lambda) \sin \theta$. λ is the wavelength of the incident radiation, and θ is equal to half the scattering angle. The film samples were fabricated by spin-coating the polymer solutions on OTS-treated silicon wafers (OTS-SiO_2/Si), followed by drying at 50 °C under vacuum.

Atomic force microscopy (AFM) (XE-100 advanced scanning probe microscope, psia) in tapping mode with a silicon cantilever was used to characterize the surface morphologies of the film samples fabricated by spin-coating (2000 rpm) the polymer solution (5 mg mL^{-1} in $CHCl_3$) on OTS-SiO_2/Si, followed by drying at 50 °C under vacuum.

To study the UV−vis absorption behavior, the thin film samples of the five polymers were fabricated on glass substrates using a solution (0.5 wt % in $CHCl_3$) of each polymer for spin-coating. The absorption spectra of the samples as thin films and as chloroform solutions were recorded on a HP 8453 photodiode array UV−vis−NIR absorption spectrometer in the 190−1100 nm range.

Fabrication and Characterization of Thin Film Transistors. For characterization of TFT performances, the BGTC device geometry was employed. The TFT devices were fabricated using n-doped Si/SiO_2 (300 nm) substrates, and n-doped Si and SiO_2 were used as the gate electrode and gate dielectric, respectively. The substrate was cleaned with acetone, a cleaning agent, deionized water, and isopropanol in an ultrasonic bath. The cleaned substrates were dried under vacuum at 120 °C for 1 h and then treated with UV/ozone for 20 min. Before the deposition of electrodes, OTS was treated with SiO_2 gate insulators to change the surface property of SiO_2/Si. The source and drain electrodes were prepared using thermal evaporation of gold (70 nm) through a shadow mask with a channel width of 1500 μm and length of 100 μm. Finally, the polymer layer was deposited on the OTS-treated substrates by spin-coating a solution (solvent: chloroform, concentration 4 mg mL^{-1}) at 2000 rpm for 30 s. To anneal the thin films in TFTs, the samples were placed on a hot plate in air at a fixed temperature for 10 min. Current−voltage characteristics of the devices were determined using a Keithley 4200 SCS semiconductor parameter analyzer in air. All the field effect mobilities were extracted in the saturation regime using the relationship $\mu_{sat} = (2I_{DS}L)/(WC(V_G - V_{th})^2)$, where I_{DS} means saturation drain current, C is the capacitance (∼11.5 nF cm^{-2}) of the SiO_2 dielectric, V_G is the gate bias, and V_{th} is the threshold voltage. Mobility data were collected from more than 15 different devices and averaged.

RL Inverter and Electrical Characterization. For the characterization of static and dynamic responses of the device, we fabricated an RL inverter, a simplified primary logic gate, by connecting the TFTs made from the five acene-containing polymers with a 20 MΩ load resistor (see Figure 5a). For the response time measurement, the input square wave gate bias was supplied by a function generator (RIGOR DG4062), and an oscilloscope (RIGOR DS2102) was connected to the output electrode to measure the output voltage signal (V_{OUT}) in air when a square wave input signal (V_{IN} = 0 to −60 V) was applied to the device at V_{DD} = −60 V.

Scheme 1. Synthesis of (a) Bis(trimethylstannyl)TTTT and (b) D−A Conjugated Polymers[a]

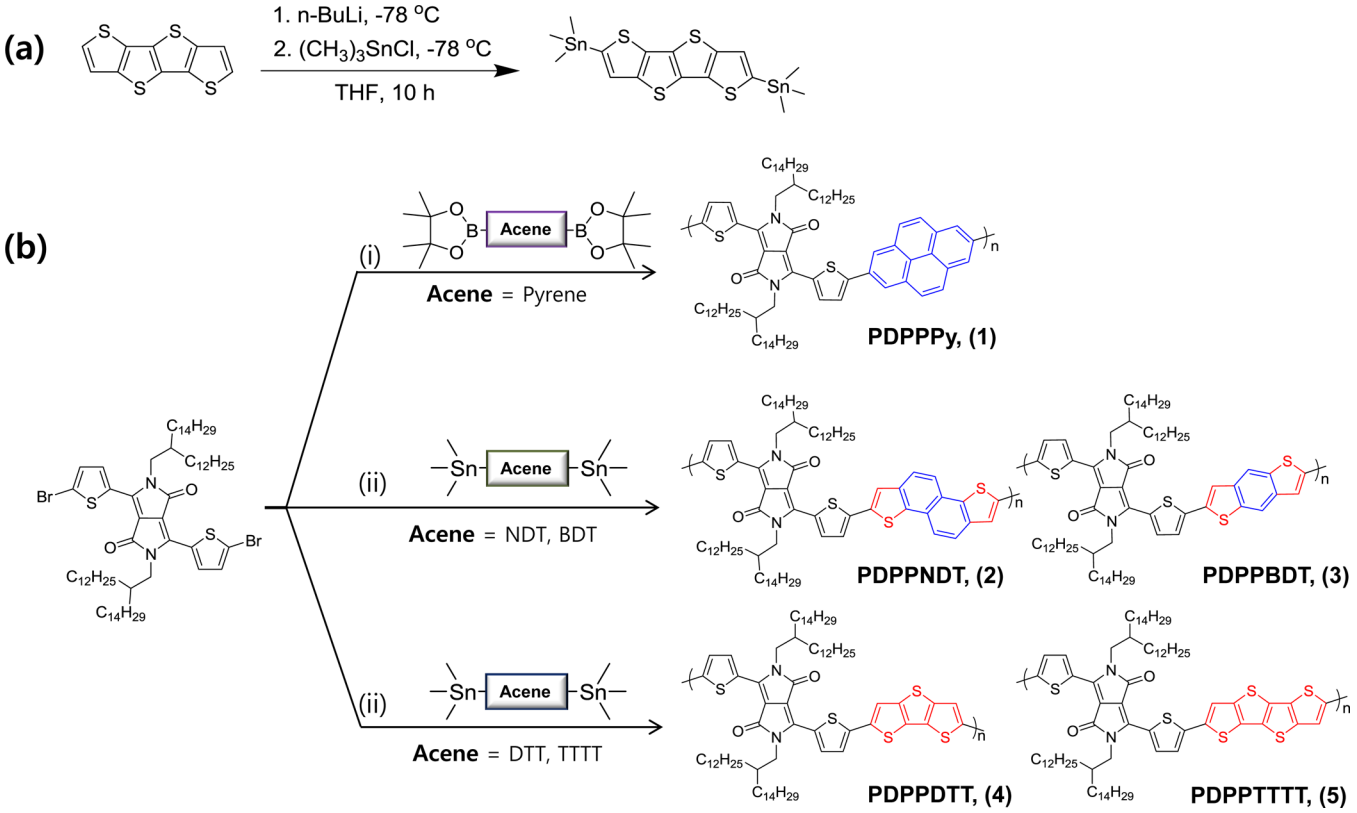

[a]Reagents and conditions: (i) $Pd_2(dba)_3$, P(*o*-tolyl)$_3$, K_2CO_3, Aliquat 336, and toluene/H_2O, 90°C; (ii) $Pd_2(dba)_3$, P(*o*-tolyl)$_3$, and toluene, 95 °C.

Table 1. Physical, Optical, and Electrochemical Properties of the Acene-Containing Conjugated Polymers

	M_n[a] (kDa)	PDI	T_d (°C)	λ_{max} (nm) solution	λ_{max} (nm) film	E_g^{opt}[b] (eV)	HOMO[c] (eV)	LUMO (eV)
PDPPPy	48.83	5.40	432	412, 696	417, 707	1.61	−5.36	−3.75
PDPPNDT	30.73	2.13	436	419, 729	428, 738	1.36	−5.34	−3.98
PDPPBDT	56.80	2.41	439	408, 745	407, 750	1.34	−5.36	−4.02
PDPPDTT	68.03	2.65	432	430, 794	437, 794	1.31	−5.22	−3.91
PDPPTTTT	58.12	2.95	433	430, 794	438, 797	1.30	−5.21	−3.91

[a]Determined by GPC with polystyrene standard. [b]Determined by onset wavelength of optical absorption. [c]Determined by cyclic voltammetry of thin films on Pt electrode. [d]LUMO = E_g^{opt} + HOMO.

RESULTS AND DISCUSSION

Synthesis and Characterization. In Scheme 1, the structures of the five different D−A conjugated polymers are displayed, including the structures of DPP-based monomers and electron-donating acene monomers. As donor monomeric units, Py, NDT, BDT, DTT, and TTTT were selected to explore the effect of acene donors on physical, optical, and molecular electronic properties of the corresponding polymers.

The polymers PDPPNDT (2), PDPPBDT (3), PDPPDTT (4), and PDPPTTTT (5) were prepared via the Stille-coupling polymerization method. On the other hand, PDPPPy (1) was prepared though the Suzuki coupling method. The resulting polymers were all purified by precipitation in methanol, followed by Soxhlet extraction to remove low molecular weight materials and undesired impurities using acetone, hexane, and chloroform, successively. The chloroform fraction was concentrated in volume, and the pure polymers were collected by precipitation in methanol in a quantitative yield

Gel permeation chromatography (GPC) measurements provided the average molecular weights (M_ns) of 48.83, 30.78, 56.80, 68.03, and 58.12 kDa for PDPPPy, PDPPNDT, PDPPBDT, PDPPDTT, and PDPPTTTT, respectively. The polydispersity index (PDI) was also determined in the range of 2.1−5.4 for the polymers (see Table 1 and Figures S1−S5 in the Supporting Information). All the synthesized polymers displayed good solubility in chloroform because of the presence of a long dodecylhexadecyl side-chain group tethered to the DPP unit.

Differential scanning calorimetry (DSC) measurements were performed at a heating (cooling) scan rate of 10 (−10) °C min^{-1} under nitrogen, with the highest temperature kept below the decomposition temperature.

Optical Absorption and Electrochemical Properties. The synthesized acene-containing conjugated polymers showed no melting behavior between 25 and 250 °C (see Figure S6a in the Supporting Information). The five polymers had great thermal stability and did not decompose at 430 °C under

dx.doi.org/10.1021/ma500733y | Macromolecules 2014, 47, 3747−3754

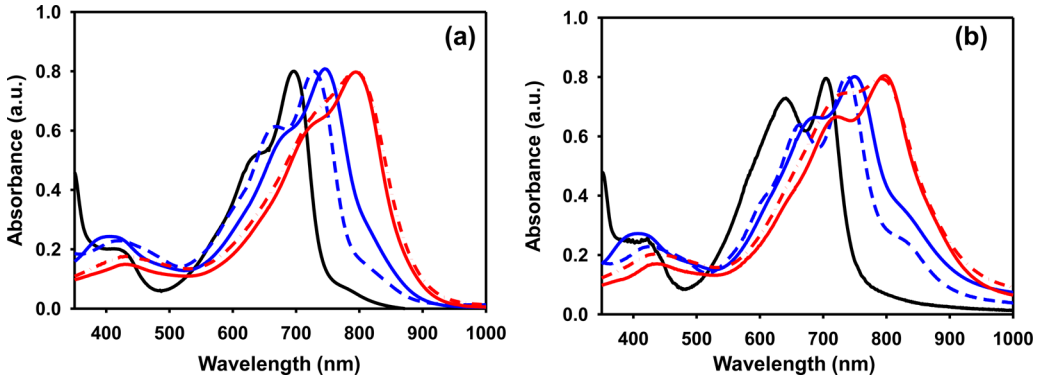

Figure 1. UV−vis absorption spectra of PDPPPy (black), PDPPNDT (blue dashed line), PDPPBDT (blue solid line), PDPPDTT (red dash-dot-dashed line), and PDPPTTTT (red solid line): (a) solutions in $CHCl_3$; (b) films.

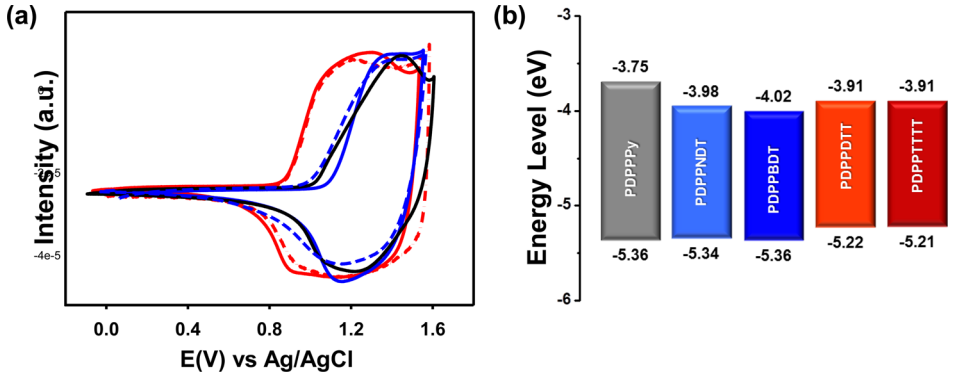

Figure 2. (a) Cyclic voltammograms and (b) the HOMO and LUMO energy levels of PDPPPy (black), PDPPNDT (blue dashed line), PDPPBDT (blue solid line), PDPPDTT (red dash-dot-dashed line), and PDPPTTTT (red solid line) films on a platinum electrode.

nitrogen, which was measured by thermogravimetric analysis (TGA) (see Figure S6b in the Supporting Information).

Figure 1 shows the absorption spectra of PDPPPy, PDPPNDT, PDPPBDT, PDPPDTT, and PDPPTTTT in chloroform solutions and films, and all the spectral data, including the maximum absorption wavelength (λ_{max}) and optical bandgap (E_g^{opt}), are summarized in Table 1. In Figure 1a, the absorption spectra of the five polymers recorded in dilute chloroform solutions display two major transition bands at 400 and 950 nm. In particular, the broad absorption band at 500−950 nm is mainly attributed to the intramolecular charge transfer (ICT) between the acceptor and donor units.[20] The absorption spectrum of PDPPPy is blue-shifted compared to those of the polymers that have both benzene and thiophene-containing comonomers such as NDT and BDT, which is attributed to shorter effective conjugation length afforded by benzene derivatives in the polymer as compared to NDT and BDT.

In addition, the PDPPDTT and PDPPTTTT polymers that have strong donor units show a red-shift of the absorption bands with respect to PDPPNDT and PDPPBDT. The absorption spectra in film states exhibit the red-shift of the maximum absorption wavelength and the absorption edges relative to the solution states. The optical bandgaps (E_g^{opt}) determined from the absorption edges of the thin films are as follows: 1.61 eV for PDPPPy, 1.36 eV for PDPPNDT, 1.34 eV for PDPPBDT, 1.31 eV for PDPPDTT, and 1.30 eV for PDPPTTTT. PDPPDTT and PDPPTTTT displayed smaller bandgaps than PDPPBDT, PDPPNDT, and PDPPPy in the films. This is likely because of the larger atomic radius of sulfur in thiophene compared to that of carbon, which can lead to stronger intermolecular interaction through the sulfur atoms.[17]

The highest occupied molecular orbital (HOMO) energy levels of the five different polymers in thin films were determined using oxidation potentials obtained from cyclic voltammetry (CV). The lowest unoccupied molecular orbital (LUMO) energy levels of the polymers were calculated by using their HOMO levels and optical bandgaps. The cyclic voltammograms of the polymers are shown in Figure 2a, and they indicate reversible oxidation behaviors. The HOMO levels of the five polymers were calculated using the onset of the oxidation potential in Figure 2b and Table 1. These results demonstrate that the replacement of benzene with thiophene in conjugated molecular frameworks of DTT and TTTT donors results in an increase in electron-donating ability, increase of HOMO level, and reduction in the bandgap.

PDPPPy showed the HOMO level of −5.36 eV and the largest bandgap, which is attributed to the twisted geometry of repeating group. PDPPNDT and PDPPBDT have similar HOMO and LUMO energy levels, and they show lower HOMO levels, −5.34 and −5.36 eV, respectively, than PDPPDTT and PDPPTTTT owing to bearing a weaker electron-donor monomers. The HOMO levels of PDPPDTT and PDPPTTTT (e.g., −5.22 and −5.21 eV) are higher than those of the other three polymers because homologous fused thiophene donors such as DTT and TTTT have stronger electron-donating ability.[21] The LUMO energy levels of five polymers exhibit no significant difference because of identical DPP acceptor monomers in the repeating group.

dx.doi.org/10.1021/ma500733y | *Macromolecules* 2014, 47, 3747−3754

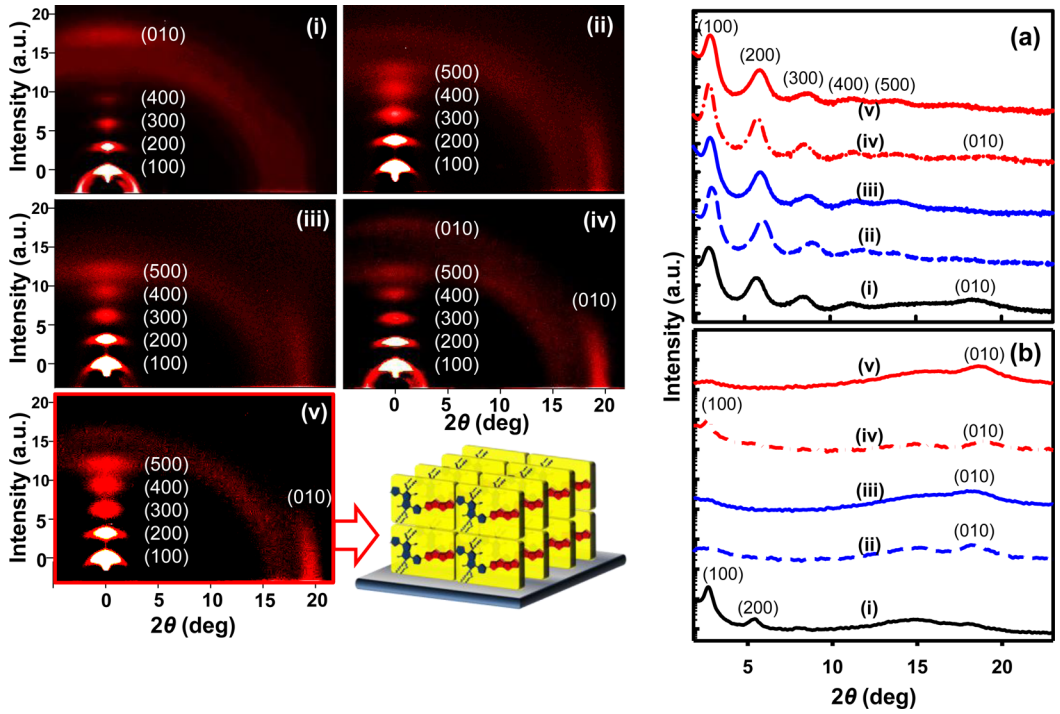

Figure 3. 2-D GI-XRD patterns and (a) out-of-plane and (b) in-plane XRD patterns of films annealed at 200 °C: (i) PDPPPy (black solid line), (ii) PDPPNDT (blue dashed line), (iii) PDPPBDT (blue solid line), (iv) PDPPDTT (red dash-dot-dashed line), and (v) PDPPTTTT (red solid line).

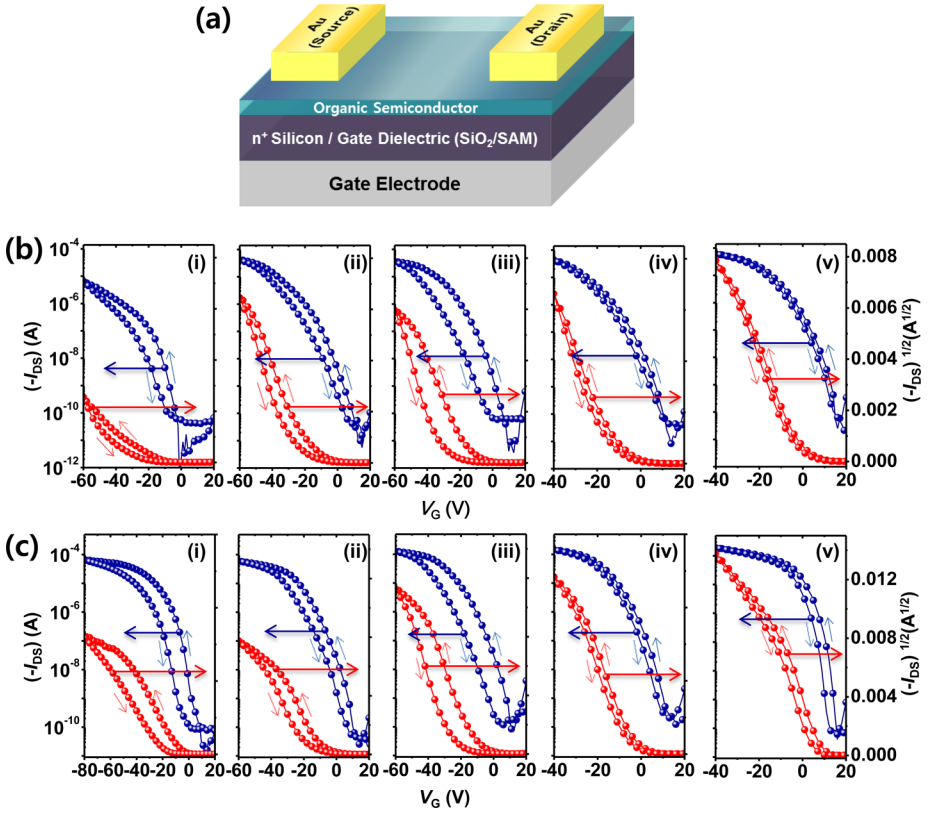

Figure 4. (a) Schematic illustration of TFT in BGTC configuration and (b) transfer characteristics at a fixed V_{DS} of −100 V for TFTs based on unannealed films made of (i) PDPPPy, (ii) PDPPNDT, (iii) PDPPBDT, (iv) PDPPDTT, and (v) PDPPTTTT. (c) Transfer characteristics at a fixed V_{DS} of −100 V for TFTs based on thermally annealed films made of (i) PDPPPy, (ii) PDPPNDT, (iii) PDPPBDT, (iv) PDPPDTT, and (v) PDPPTTTT. Annealing temperature: 200 °C.

GI-XRD and AFM Analysis of the Polymer Thin Films. To investigate the influence of thin film morphology and surface topographies of these polymers on TFT performances, the 2-dimensional X-ray diffraction (2-D XRD) patterns, out-

dx.doi.org/10.1021/ma500733y | Macromolecules 2014, 47, 3747−3754

of-plane, and in-plane profiles of polymer thin films for acene-containing conjugated polymers were obtained from GI-XRD analysis (see Figure 3 and Table S1). The thermally annealed thin films on the *n*-octyltrichlorosilane (OTS)-modified SiO_2/Si substrate exhibited a relatively high intensity (100) diffraction peak and well-resolved, high-order diffraction peaks compared to those of the as-cast thin films (Figure S7 in the Supporting Information). For a precise comparison, the diffractograms of the five polymers exhibited (100) peaks at 2θ = 2.88°−3.08°, corresponding to the d(100)-spacing values of 21.68−23.15 Å. Each polymer gave distinct diffraction features in the out-of-plane direction shown in Figure 3a. In particular, it was clearly observed that PDPPTTTT does not exhibit (010) diffraction in an out-of-plane profile (curve v). In an in-plane profile, the (100) diffraction peak did not appear, and (010) diffraction from the π−stacking distance was only resolved with a high intensity (2θ = 18.6°, d(010) = 3.60 Å) (Figure 3a,b, curve v). This indicates PDPPTTTT chains are predominantly arranged in an edge-on manner on the OTS-SiO_2/Si substrate. Even in the 2-D XRD of unannealed PDPPTTTT film, higher order (h00) and (010) diffraction peaks were more clearly observed compared to the other four polymers (Figure S7 in the Supporting Information).

On the other hand, the out-of-plane diffraction of PDPPPy exhibited (100) and (010) diffraction peaks together. In an in-plane profile, (100) and (200) diffraction peaks were also observed without having a clear (010) diffraction peak. This indicates that the PDPPPy polymer chains were arranged in a face-on manner rather than edge-on orientation on the substrate (curve i, Figure 3a,b).

Besides two polymers, PDPPNDT, PDPPBDT, and PDPPDTT also exhibited highly resolved (h00) diffraction peaks to the fifth order in an out-of plane profile, and faint (010) diffraction peaks could be observed in an in-plane profile. Three polymers, PDPPNDT, PDPPBDT, and PDPPDTT, also showed the edge-on orientation of polymer chains on the substrate predominantly over the face-on orientation. Therefore, it was concluded that the polymer containing a homologous heteroaromatic donor unit, TTTT, displays the most favorable π−π stacking and prominent edge-on orientation on the substrate. It might affect the charge transport property, resulting in an increase of carrier mobility in TFTs.

The thin film morphologies of acene-containing conjugated polymers were investigated using tapping-mode AFM. The film was thermally annealed at 200 °C, and the five polymers displayed highly dense surface morphologies in which densely connected small crystallites covered the surface uniformly (Figure S8 in the Supporting Information). It was considered that the planar DPP and acene monomers contributed to the high crystallinity, and highly dense small crystallites formed to occupy the surface of OTS-SiO_2/Si. The connectivity between neighboring crystallite domains is highly improved after thermal annealing, which can facilitate the building of efficient pathways for charge transport and enhance the charge mobility in a TFT device.

Electrical Properties of TFTs. Electrical properties of acene-containing conjugated polymers were investigated by fabricating TFT devices in a bottom gate top contact (BGTC) configuration (see Figure 4a). All the devices were measured under ambient conditions. The mobility (μ) and threshold voltage (V_{th}) were calculated from the saturation regimes. The performances of fabricated TFTs are summarized in Table 2, and the representative transfer characteristics of polymer thin films before and after annealing at 200 °C are shown in Figure 4b,c.

Table 2. Device Performance of Solution-Processed TFTs on Acene-Containing Conjugated Polymers

polymer	$T_{annealing}$ (°C)	μ_{ave} [$cm^2\ V^{-1}\ s^{-1}$]	μ_{max}[a] [$cm^2\ V^{-1}\ s^{-1}$]	I_{on}/I_{off}	V_{th} [V]
PDPPPy	as-cast	0.04	0.08	$>10^6$	−9
	200	0.46	0.68	$>10^7$	−5
PDPPNDT	as-cast	0.26	0.42	$\sim10^7$	−14
	200	0.54	0.78	$\sim10^7$	−7
PDPPBDT	as-cast	0.27	0.45	$>10^7$	−12
	200	0.86	1.31	$>10^6$	−7
PDPPDTT	as-cast	0.55	1.18	$>10^6$	−10
	200	1.42	2.31	$\sim10^6$	−1
PDPPTTTT	as-cast	0.70	1.19	$\sim10^6$	0
	200	2.22	3.20	$>10^6$	8

[a]Gate voltage ranges for determining the saturated mobilities: (b) (i) −29 to −58 V, (ii) −30 to −50 V, (iii) −22 to −46 V, (iv) −16 to −36 V, (v) −5 to −26 V; (c) (i) −12 to −47 V, (ii) −14 to −34 V, (iii) −18 to −39 V, (iv) −7 to −23 V, (v) +8 to −10 V.

Their TFT characteristics were found to be largely dependent on the electron-donor moiety in the repeating group. The as-cast thin film of PDPPPy exhibited a mobility of 0.08 $cm^2\ V^{-1}\ s^{-1}$ with a current on/off ratio of $>10^6$ (Figure 4b(i)). The mobility of PDPPPy thin films increased up to 0.68 $cm^2\ V^{-1}\ s^{-1}$ with a high on/off ratio of $>10^7$ after thermal annealing at 200 °C. The as-cast film in TFT showed a mobility of 0.42 $cm^2\ V^{-1}\ s^{-1}$ for PDPPNDT (Figure 4b(ii)) and 0.45 $cm^2\ V^{-1}\ s^{-1}$ for PDPPBDT (Figure 4b(iii)). After thermal annealing at 200 °C, the carrier mobilities were improved to 0.78 (Figure 4c(ii)) and 1.31 $cm^2\ V^{-1}\ s^{-1}$ (Figure 4c(iii)), respectively, with a high current on/off ratio of $>10^6$.

From the results of TFT characterization, it was found that the charge transport property was improved by adding more electron-rich thiophene units to the aromatic donor moiety. Among the five polymers, PDPPDTT and PDPPTTTT polymers were found to exhibit higher mobility in TFTs than the others. In the case of PDPPDTT, the as-cast films showed a mobility of 1.18 $cm^2\ V^{-1}\ s^{-1}$ (Figure 4b(iv)). The carrier mobility was enhanced to 2.31 $cm^2\ V^{-1}\ s^{-1}$ after thermal annealing at 200 °C (Figure 4c(iv)). Particularly, PDPPTTTT containing four thiophene fused heteroaromatic ring moieties exhibited the highest hole mobility of ~3.2 $cm^2\ V^{-1}\ s^{-1}$ (I_{on}/I_{off} > 10^6) after thermal annealing at 200 °C (Figure 4c(v)) (i.e., μ = 1.19 $cm^2\ V^{-1}\ s^{-1}$, obtained from as-cast film (Figure 4b(v)). The highest mobility of PDPPTTTT is prominently ascribed to the perfectly planar structure of TTTT and the almost perfect edge-on orientation of the polymers chains on OTS-SiO_2/Si substrates. Therefore, the donor moiety in the repeating unit can govern the geometry of repeating group, molecular electronic property, solid-state morphology, and charge transport property of the polymer.

Characterization of the Resistor Loaded (RL) Inverter: Charge Transport Dynamics. To investigate the static and dynamic response of the TFTs, simple RL inverters were built by connecting a load resistor (20 MΩ) as shown in Figure 5a. The dynamic response behaviors of the inverters made of the acene-containing polymer-based TFTs at a frequency of 10 Hz are shown in Figure 5b. Although the device structures were

dx.doi.org/10.1021/ma500733y | Macromolecules 2014, 47, 3747−3754

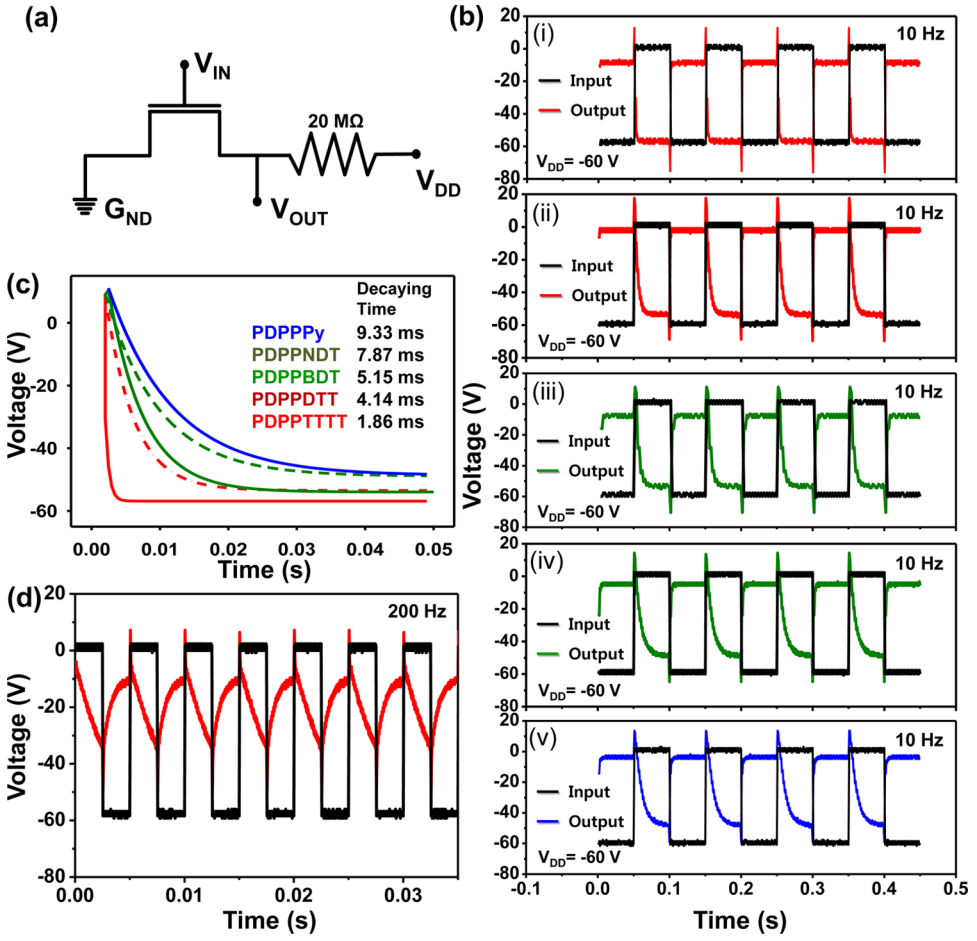

Figure 5. RL inverters made of acene-containing conjugated polymers. (a) Circuit diagram of RL inverter. (b) Dynamic output voltage response of five DPP polymer-based inverters. Output responses when the input voltage was switched at 10 Hz. (i) PDPPTTTT, (ii) PDPPDTT, (iii) PDPPBDT, (iv) PDPPNDT, and (v) PDPPPy (c) Decay curves of the input signal after turning off the TFTs. The decay times are shown in the figure. (d) Output response of PDPPTTTT polymer-based RL inverter when the square wave input voltage was switched at 200 Hz. At a 200 Hz input voltage signal, the inverter still operated well, maintaining complete output switching. *W = 1500 μm, L = 100 μm.

not optimized to promote a switching response, all the devices exhibited a decent switching behavior with different response times, as shown in Figure 5c. As can be seen in Figure 5b, when the square wave input bias (V_{IN}) is applied at 10 Hz, the output voltage (V_{OUT}) was switched from the ON to OFF state and vice versa in the inverters made of the five polymers.

To investigate the relationship between carrier mobility and dynamic response, we measured the switching response time of RL inverters with a 10 Hz input voltage signal. The decay time was determined by fitting the curve from the ON to OFF state to a single-exponential decay function. The rising times of all the devices at 10 Hz were smaller than 1 ms. However, there was a significant difference in the decay time between the devices made from the five polymers.

As can be seen in Figure 5c, the PDPPPy-based device had a decay time of 9.33 ms. However, the decay time of the PDPPTTTT-based inverter to the OFF state was 1.86 ms, which is much smaller than those of the others. The response times of the PDPPTTTT-based inverter were also found to be markedly shorter than that of the poly(3-hexylthiophene) (P3HT)-based inverter with an identical device configuration (mobility of P3HT = $\sim 5 \times 10^{-3}$ cm^2 V^{-1} s^{-1}, τ = 15.7 ms at 10 Hz in Figure S14 of the Supporting Information).

The order of the decay time is consistent with the order of carrier mobility in static states. The dynamic response of the inverter made of PDPPTTTT was examined at various frequencies of V_{IN}, as shown in Figure S15 (Supporting Information). The inverter made of PDPPTTTT operates well, maintaining a fairly high switching voltage ratio ($V_{out}^{ON}/V_{out}^{OFF}$) at a higher frequency of 200−500 Hz (Figure S16).

CONCLUSION

In this study, five acene-containing π-conjugated polymers were successfully synthesized via the Suzuki and Stille coupling methods. The polymers contain diketopyrrolopyrrole as an acceptor unit and fused-acene donor units, Py, NDT, BDT, DTT, and TTTT.

Among the five acene-based polymers, PDPPTTTT exhibited the highest hole mobility, ~3.2 cm^2 V^{-1} s^{-1} (I_{on}/I_{off} > 10^6), in a TFT device owing to the planar structure along the polymer backbone and a prominent edge-on orientation of the polymer chains on OTS-SiO_2/Si substrates. The dynamic response behaviors of the RL inverters based on the five acene-containing polymers were investigated at a frequency of 10 Hz. At this frequency, all polymers displayed sufficient switching responses. Among the five RL inverters, the PDPPTTTT-based device had a response time of 1.86 ms for switching from the ON to OFF state, which is much smaller than those of the others. It was found that the RL-inverter made of PDPPTTTT operates well and maintains a fairly high switching voltage ratio

dx.doi.org/10.1021/ma500733y | Macromolecules 2014, 47, 3747−3754

at a higher frequency of 200−500 Hz. It should be noted that the response time of the polymer-based TFT should be improved by optimizing device structures and developing higher performance conjugated polymers for practical application to commercial industry.

It was unambiguously demonstrated that the structure of the donor moiety in the D−A conjugated polymer could strongly affect the internal morphology of the polymer film, charge carrier mobility in TFT, and charge transport dynamics in corresponding inverter devices.

■ ASSOCIATED CONTENT

Supporting Information

GPC, FT-IR, NMR, TGA, DSC, and GI-XRD patterns of unannealed films, AFM height images, output and transfer curves of TFTs, more data obtained from the resistor-loaded (RL) inverters, etc. This material is available free of charge via the Internet at http://pubs.acs.org.

■ AUTHOR INFORMATION

Corresponding Authors

*E-mail pyosm@konkuk.ac.kr (S.P).
*E-mail dhchoi8803@korea.ac.kr (D.H.C.).

Notes

The authors declare no competing financial interest.

■ ACKNOWLEDGMENTS

This research was supported by National Research Foundation of Korea (NRF2012R1A2A1A01008797) and by Key Research Institute Program (NRF201200020209). We are grateful to Pohang Accelerator Laboratory (Pohang, Korea) for allowing us to conduct the grazing incidence X-ray diffraction (GI-XRD) measurements.

■ REFERENCES

(1) (a) Yi, H. T.; Payne, M. M.; Anthony, J. E.; Podzorov, V. *Nat. Commun.* **2012**, *3*, 1259. (b) Sirringhaus, H. *Adv. Mater.* **2014**, *26*, 1319. (c) Baeg, K.-J.; Caironi, M.; Noh, Y.-Y. *Adv. Mater.* **2013**, *25*, 4210. (d) Yan, H.; Chen, Z.; Zheng, Y.; Newman, C.; Quinn, J. R.; Dötz, F.; Kastler, M.; Facchetti, A. *Nature* **2009**, *457*, 679.

(2) (a) Nielsen, C. B.; Turbiez, M.; McCulloch, I. *Adv. Mater.* **2013**, *25*, 1859. (b) Li, Y.; Sonar, P.; Singh, S. P.; Soh, M. S.; van Meurs, M.; Tan, J. *J. Am. Chem. Soc.* **2011**, *133*, 2198. (c) Yi, Z.; Sun, X.; Zhao, Y.; Guo, Y.; Chen, X.; Qin, J.; Yu, G.; Liu, Y. *Chem. Mater.* **2012**, *24*, 4350.

(3) (a) Tsao, H. N.; Cho, D. M.; Park, I.; Hansen, M. R.; Mavrinskiy, A.; Yoon, D. Y.; Graf, R.; Pisula, W.; Spiess, H. W.; Müllen, K. *J. Am. Chem. Soc.* **2011**, *133*, 2605. (b) Kim, J.; Baeg, K.-J.; Khim, D.; James, D. T.; Kim, J.-S.; Lim, B.; Yun, J.-M.; Jeong, H.-G.; Amegadze, P. S. K.; Noh, Y.-Y.; Kim, D.-Y. *Chem. Mater.* **2013**, *25*, 1572. (c) Zhao, Z.; Zhang, F.; Zhang, X.; Yang, X.; Li, H.; Gao, X.; Di, C.; Zhu, D. *Macromolecules* **2013**, *46*, 7705.

(4) (a) Kim, Y.; Hong, J.; Oh, J. H.; Yang, C. *Chem. Mater.* **2013**, *25*, 3251. (b) Luzio, A.; Fazzi, D.; Natali, D.; Giussani, E.; Baeg, K.-J.; Chen, Z.; Noh, Y.-Y.; Facchetti, A.; Caironi, M. *Adv. Funct. Mater.* **2013**, *24*, 1151. (c) Li, J.; Zhao, Y.; Tan, H. S.; Guo, Y.; Di, C.-A.; Yu, G.; Liu, Y.; Lin, M.; Lim, S. H.; Zhou, Y.; Su, H.; Ong, B. S. *Sci. Rep.* **2012**, *2*, 754. (d) Hu, X.; Fu, W.; Zuo, L.; Shi, H.; Chen, M.; Liu, S.; Pan, J.; Fu, L.; Shi, M.; Chen, H. *Tetrahedron* **2013**, *69*, 3419.

(5) Yi, Z.; Ma, L.; Chen, B.; Chen, D.; Chen, X.; Qin, J.; Zhan, X.; Liu, Y.; Ong, W. J.; Li, J. *Chem. Mater.* **2013**, *25*, 4290.

(6) (a) Sonar, P.; Singh, S. P.; Li, Y.; Ooi, Z.-E.; Ha, T.-J.; Wong, I.; Soh, M. S.; Dodabalapur, A. *Energy Environ. Sci.* **2011**, *4*, 2288. (b) Yang, D. S.; Kim, K. H.; Cho, M. J.; Jin, J.-I.; Choi, D. H. *J. Polym. Sci., Part A: Polym. Chem.* **2013**, *51*, 1457. (c) Uemura, T.; Mamada, M.; Kumaki, D.; Tokito, S. *ACS Macro Lett.* **2013**, *2*, 830.

(7) Lee, T. W.; Lee, D. H.; Shin, J.; Cho, M. J.; Choi, D. H. *J. Polym. Sci., Part A: Polym. Chem.* **2013**, *51*, 5280.

(8) (a) Osaka, I.; Abe, T.; Shinamura, S.; Miyazaki, E.; Takimiya, K. *J. Am. Chem. Soc.* **2010**, *132*, 5000. (b) Shi, S.; Xie, X.; Gao, C.; Shi, K.; Chen, S.; Yu, G.; Guo, L.; Li, X.; Wang, H. *Macromolecules* **2014**, *47*, 616.

(9) Osaka, I.; Kakara, T.; Takemura, N.; Koganezawa, T.; Takimiya, K. *J. Am. Chem. Soc.* **2013**, *135*, 8834.

(10) (a) Han, Y.; Chen, L.; Chen, Y. *J. Polym. Sci., Part A: Polym. Chem.* **2013**, *51*, 258. (b) Jung, J. W.; Jo, J. W.; Liu, F.; Russell, T. P.; Jo, W. H. *Chem. Commun.* **2012**, *48*, 6933. (c) Zhang, G.; Fu, Y.; Qiu, L.; Xie, Z. *Polymer* **2012**, *53*, 4407.

(11) Li, Z.; Zhang, Y.; Tsang, S.-W.; Du, X.; Zhou, J.; Tao, Y.; Ding, J. *J. Phys. Chem. C* **2011**, *115*, 18002.

(12) (a) Shahid, M.; Ashraf, R. S.; Huang, Z.; Kronemeijer, A. J.; McCarthy-Ward, T.; Maculloch, I.; Durrant, J. R.; Sirringhaus, H.; Heeney, M. *J. Mater. Chem.* **2012**, *22*, 12817. (b) Jung, J. W.; Liu, F.; Russell, T. P.; Jo, W. H. *Energy Environ. Sci.* **2012**, *5*, 6857.

(13) (a) Patil, A. V.; Lee, W.-H.; Kim, K.; Park, H.; Kang, I. N.; Lee, S.-H. *Polym. Chem.* **2011**, *2*, 2907. (b) Ku, S.-Y.; Liman, C. D.; Burke, D. J.; Treat, N. D.; Cochran, J. E.; Amir, E.; Perez, L. A.; Chabinyc, M. L.; Hawker, C. J. *Macromolecules* **2011**, *44*, 9533.

(14) Liu, Y.; Wang, Y.; Wu, W.; Liu, Y.; Xi, H.; Wang, L.; Qiu, W.; Lu, K.; Du, C.; Yu, G. *Adv. Funct. Mater.* **2009**, *19*, 772.

(15) (a) Matthews, J. R.; Niu, W.; Tandia, A.; Wallace, A. L.; Hu, J.; Lee, W.-Y.; Giri, G.; Mannsfeld, S. C. B.; Xie, Y.; Cai, S.; Fong, H. H.; Bao, Z.; He, M. *Chem. Mater.* **2013**, *25*, 782. (b) Lee, W.-Y.; Giri, G.; Diao, Y.; Tassone, C. J.; Matthews, J. R.; Sorensen, M. L.; Mannsfeld, S. C. B.; Chen, W.-C.; Fong, H. H.; Tok, J. B.-H.; Toney, M. F.; He, M.; Bao, Z. *Adv. Funct. Mater.* **2014**, DOI: 10.1002/adfm.201303794.

(16) (a) Mazaki, Y.; Kobayashi, K. *Tetrahedron Lett.* **1989**, *30*, 3315. (b) Zhang, X.; Johnson, J. P.; Kampf, J. W.; Matzger, A. J. *Chem. Mater.* **2006**, *18*, 3470.

(17) Takimiya, K.; Shinamura, S.; Osaka, I.; Miyazaki, E. *Adv. Mater.* **2011**, *23*, 4347.

(18) (a) Shin, J.; Um, H. A.; Lee, D. H.; Lee, T. W.; Cho, M. J.; Choi, D. H. *Polym. Chem.* **2013**, *4*, 5688. (b) Lee, J. S.; Son, S. K.; Song, S.; Kim, H.; Lee, D. R.; Kim, K.; Ko, M. J.; Choi, D. H.; Kim, B.; Cho, J. H. *Chem. Mater.* **2012**, *24*, 1316. (c) Rieger, R.; Beckmann, D.; Pisula, W.; Kastler, M.; Müllen, K. *Macromolecules* **2010**, *43*, 6264. (d) Deng, Y.; Chen, Y.; Zhang, X.; Tian, H.; Bao, C.; Yan, D.; Geng, Y.; Wang, F. *Macromolecules* **2012**, *45*, 8621.

(19) (a) Cho, J. H.; Lee, J.; Xia, Y.; Kim, B.; He, Y.; Renn, M. J.; Lodge, T. P.; Frisbie, C. D. *Nat. Mater.* **2008**, *7*, 900. (b) Cho, J. H.; Lee, J.; He, Y.; Kim, B.; Lodge, T. P.; Frisbie, C. D. *Adv. Mater.* **2008**, *20*, 686. (c) Lee, J.; Kaake, L. G.; Cho, J. H.; Zhu, X.-Y.; Lodge, T. P.; Frisbie, C. D. *J. Phys. Chem. C* **2009**, *113*, 8972. (d) Kawase, T.; Sirringhaus, H.; Friend, R. H.; Shimoda, T. *Adv. Mater.* **2001**, *13*, 1601. (e) Sirringhaus, H.; Kawase, T.; Friend, R. H.; Shimoda, T.; Inbasekaran, M.; Wu, W.; Woo, E. P. *Science* **2000**, *290*, 2123.

(20) Henson, Z. B.; Welch, G. C.; van der Poll, T.; Bazan, G. C. *J. Am. Chem. Soc.* **2012**, *134*, 3766.

(21) Choi, Y. S.; Jo, W. H. *Org. Electron.* **2013**, *14*, 1621.